

Thermal Activation in a Two-Dimensional Potential

S. Han, J. Lapointe, and J. E. Lukens

Department of Physics, State University of New York at Stony Brook, Stony Brook, New York 11794

(Received 13 July 1989)

Measurements have been made of the transition rates between fluxoid states of a system with two Josephson junctions having two macroscopic degrees of freedom. The data, taken over a temperature range of 0.85 to 4.41 K, are in excellent agreement with the predictions for thermally activated transitions. No evidence is seen for recently reported apparent rate suppression below that predicted for thermal activation.

PACS numbers: 74.50.+r, 05.40.+j, 85.25.Cp

Josephson junctions have proven to be excellent systems in which to study the dynamics, both classical and quantum, of a macroscopic coordinate in a metastable potential. In general, careful experiments have yielded excellent agreement with theory for systems with one degree of freedom, i.e., a single, small junction. Recent results by Sharifi, Gavilano, and Van Harlingen^{1,2} (SGV) on thermal activation from the zero-voltage state of a dc SQUID (a system with two degrees of freedom) have, however, shown marked disagreement with classical theory for two-dimensional (2D) potentials and have been interpreted as showing a dramatic suppression of the thermal activation rate from that predicted. In this Letter we report the results of thermal activation measurements on a similar two-dimensional system of Josephson junctions (a combined rf-dc SQUID) in which the potential can be independently determined to very high accuracy.

The system studied here, as shown in Fig. 1, consists of two Josephson junctions in parallel in a low inductance (l) superconducting loop (the dc SQUID) which is incorporated as part of a larger inductance (L) superconducting loop (the rf SQUID). The macroscopic dynamical variables which describe this system are the fluxes Φ (which can be monitored) and Φ_{dc} linking, respectively, the rf and dc SQUID's. The fluxes applied to these loops, Φ_x and $\Phi_{x,dc}$, can be independently controlled. The dynamics of this system can be visualized as motion in a 2D potential, which for symmetric dc SQUID having equal junctions is given by

$$U(\varphi, \varphi_{dc}) = \frac{\Phi_0^2}{4\pi^2 L} \left[\frac{1}{2} (\varphi - \varphi_x)^2 + \frac{1}{2} \gamma (\varphi_{dc} - \varphi_{x,dc})^2 - \beta \cos \frac{1}{2} \varphi_{dc} \cos \varphi \right], \quad (1)$$

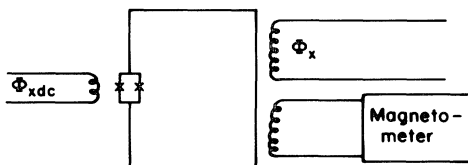


FIG. 1. Schematic of SQUID sample and coupling coils.

with a damping determined both by the junctions' resistance and the environment. Here, Φ_0 is the flux quantum, $\gamma \equiv L/l$ is the ratio of the loop inductances, and $\beta \equiv 2\pi L I_c / \Phi_0$, where I_c is the sum of the junctions' critical currents. $\varphi(\Phi) = \Phi(\Phi) [2\pi/\Phi_0]$. Figure 2 shows a plot of this potential for $\beta = 4.14$ and $\gamma = 19.5$ (the case for the junctions measured here) with $\Phi_x = 0.65\Phi_0$ and $\Phi_{x,dc} = 0$. For these parameters the potential consists of two local minima connected by a saddle point. For the values of β and γ here, there are at most two local minima with $U(\Phi, \Phi_{dc})$ increasing roughly parabolically at large Φ and Φ_{dc} . For values of $\Phi_{x,dc} > 0$ the barrier amplitude is reduced, finally going to zero for $\Phi_{x,dc} = 0.405\Phi_0$ (for

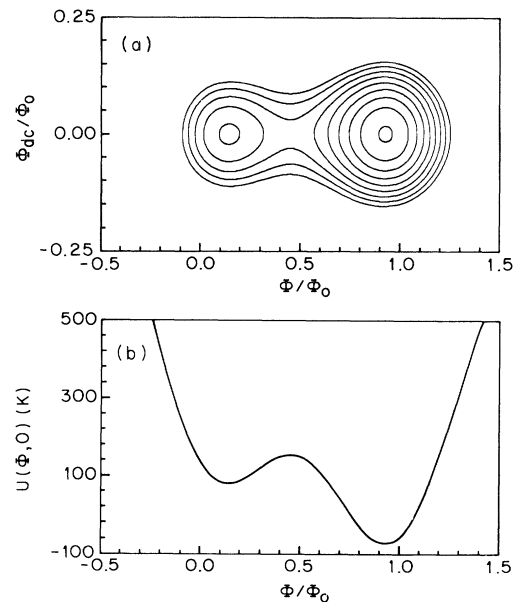


FIG. 2. The 2D potential $U(\Phi, \Phi_{dc})$ of our sample SQUID with symmetric dc SQUID having identical junctions. The mutual inductance between two loops is taken to be $l/2$. The potential for $\beta = 4.14$, $\gamma = 19.5$, $\Phi_x = 0.65\Phi_0$, and $\Phi_{x,dc} = 0$ showing (a) equipotential contours at the above value of external fluxes and (b) $U(\Phi, 0)$. U continues to increase monotonically (roughly parabolically) for greater values of Φ and Φ_{dc} than those shown.

$\Phi_x = \frac{1}{2}\Phi_0$) so that no metastable states exist. Also for $\Phi_{x\text{dc}} > 0$ the path linking the wells through the saddle point is no longer a straight line. The details of this potential along with the techniques used for the measurement of its parameters will be presented in a forthcoming extended paper.

The longitudinal (transverse) small oscillation frequencies parallel (perpendicular) to the path from the well through the saddle point are ω_{lw} (ω_{tw}) in the well and ω_{ls} (ω_{ts}) at the saddle point. The predicted rate of thermally activated escape from such a two-dimensional well is given in the classical limit by Ben-Jacob *et al.*³ to be

$$\Gamma_{2D} = \frac{\Omega}{2\pi} \exp[-\Delta U(\varphi, \varphi_{\text{dc}})/k_B T], \quad (2)$$

where ΔU is the energy difference between the metastable potential well and the saddle point and $\Omega = \Omega_0 a_t$, $\Omega = \omega_{\text{lw}}\omega_{\text{tw}}/\omega_{\text{ts}}$ and a_t is a damping-dependent suppression of the rate which can be much less than one in both high- and low-damping limits, i.e., for ω much greater or much less than RC . R and C are, respectively, the junction's resistance and capacitance. For moderate to heavy damping $a_t = (1 + G^2/4) - G/2$, where $G = 1/RC\omega_{\text{ls}}$. In the extreme underdamped limit, $a_t \ll 1$ is also predicted since

$$a_t = \frac{2\pi\omega_{\text{ts}}}{\omega_{\text{tw}}} \frac{1}{RC\omega_{\text{lw}}} \left(\frac{\Delta U}{k_B T} \right)^2.$$

Recent results for single-current biased junctions provide evidence for this extreme underdamped limit with a damping $\eta \propto \exp(-\Delta U/k_B T)$, where ΔU is the superconducting energy gap, as expected for quasiparticles.⁴⁻⁶ However, the extension of these results to multidimensional potentials is still open to question.⁷

All measurements were made in highly shielded cryostats (either ⁴He or dilution refrigerator). All signals were inductively coupled to the sample, which was enclosed in a NbTi can, through leads having low-temperature low-pass filters. For low-temperature measurements a resistive shunt, heat sunk to the dilution refrigerator mixing chamber, was placed across the magnetometer input to filter any high-frequency signals generated by the SQUID magnetometer. The junctions used were nominal $1 \times 1 \mu\text{m}^2$ Nb/Al₂O₃/Nb tunnel junctions with very low subgap leakage. The I - V curve of an unshunted (without L) SQUID coprocessed with the sample SQUID is shown in the inset of Fig. 3(b). These data give a single-junction differential resistance of $R_n = 320 \Omega$ above the gap and a critical current of $I_c = 5.8 \mu\text{A}$. From the dc SQUID resonance of this unshunted SQUID with $\Phi_{x\text{dc}} > 0$, a capacitance of $C = 46 \pm 6$ fF was determined in agreement with the specific capacitance obtained by Lichtenberger *et al.* for similar junctions.⁸ The inductance l of the dc SQUID was determined from the sample as discussed below.

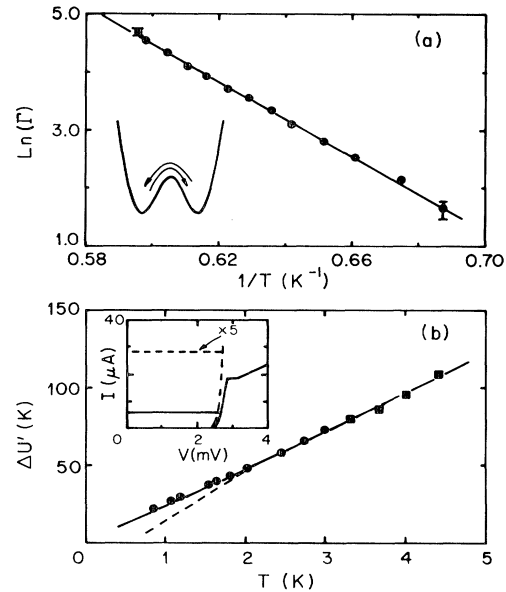


FIG. 3. Thermal activation rates between fluxoid states for the symmetric potential ($\Phi_x = \frac{1}{2}\Phi_0$) shown as the inset in (a). (a) Rate vs $1/T$ for fixed barrier height with best linear fit (line). (b) Barrier height vs T for fixed rate ($\Gamma = 1 \text{ s}^{-1}$). For points indicated by squares, data have been corrected for temperature dependence of critical current. Best fit by Eq. (2) assuming damping due to R_n (solid line), or damping proportional to $\exp[-\Delta U/k_B T]$ from quasiparticles (dashed line). The inset of (b) shows the dc SQUID I - V curve for $T = 1.5 \text{ K}$, $\Phi_{x\text{dc}} = 0$ indicating low subgap leakage.

For the special case where Φ_x is a half-integer flux quantum, the potential is symmetric about $\Phi = \Phi_x$ so that $\Delta U(\Phi_{x\text{dc}})$ is the same for each well [see inset, Fig. 3(a)], varying from a maximum of 143 K for $\Phi_{x\text{dc}} = 0$ to 0 for $\Phi_{x\text{dc}} > 0.405\Phi_0$, where the potential has only one minimum. Figure 3(a) shows the measured rate at which the sample hops between two equal energy fluxoid states versus temperature with constant ΔU (fixed $\Phi_{x\text{dc}}$). If Ω is temperature independent in this range, one expects from Eq. (2) that a linear relationship exists between $\ln(\Gamma)$ and $1/T$ since

$$\ln(\Gamma) = -\Delta U/kT + \ln(\Omega/2\pi). \quad (3)$$

As Fig. 3 shows, the observed dependence is in fact linear, giving best-fit values of $\Delta U = 32.2 \pm 0.4 \text{ K}$ and $\ln(\Omega/2\pi) = 23.9 \pm 0.3$. These agree well with the values of $\Delta U = 33.5 \pm 3 \text{ K}$ and $\ln(\Omega/2\pi) = 24.4 \pm 0.2$ calculated from measured sample parameters, as discussed below. Here $a_t = 1$ has been used; taking the damping to be $1/R_n$ would give $a_t \approx 0.9$ —an insignificant correction.

The greatest uncertainty in the calculated value of ΔU comes from the knowledge of L , which has been calculated from the loop geometry, giving $L = 230 \text{ pH} \pm 10\%$. Measurements on single-junction SQUID's^{9,10} have shown such calculations to be reliable for the geometry

used here. Both γ and the difference in the junctions' critical currents, $\delta \equiv (I_2 - I_1)/I_c$, can be determined from the equilibrium dependence of Φ on Φ_x measured when Φ_{xdc} is a half-integer flux quantum so that the system has no metastable states. These data give $\gamma = 19.5$ and $\delta < 5\%$ justifying the treatment of the junction parameters as equal. β is determined by measuring the value of Φ_x at which the system escapes from its metastable state for $\Phi_{xdc} = 0$. Since this escape will occur slightly before the barrier is reduced to zero, a small, model-dependent correction to β based on Eq. (2) is required. This correction, at most, increases the calculated ΔU above by 5% over that which would be obtained by assuming the escape occurred for $\Delta U = 0$.

The transition rate as shown in Fig. 3(a) is only measurable over a narrow range of temperature for fixed ΔU . To measure the temperature dependence of this rate over a broad range of temperature, ΔU was adjusted at each temperature to give approximately the same rate, $10 < \Gamma < 50$. These data are plotted as $\Delta U'$ vs T in Fig. 3(b). Here $\Delta U' \equiv \Delta U + k_B T \ln[\Gamma/1 \text{ s}^{-1}]$ is the measured barrier normalized for the small variations in $\ln(\Gamma)$ among the points. Again $\Phi_x = \frac{1}{2}\Phi_0$ and $\Delta U(\Phi_{xdc})$ was adjusted by varying Φ_{xdc} and calculated from the parameters as above.

The theoretical curve for thermal activation has been plotted using Eq. (3) taking the damping to be $1/R_n$ which gives $a_t \approx 0.9$. The uncertainty in the independently measured values of $\Delta U \pm 10\%$ implies an acceptable fit to the data in Fig. 3(b) for any temperature-independent damping less than $0.05 \Omega^{-1}$ if the moderate damping expression for a_t is used. The dashed line in Fig. 3(b) is calculated assuming the damping $\eta \propto \exp(-\Delta U/k_B T)$ as expected for quasiparticles and using the extreme underdamped expression for a_t . This is not consistent with our data; however, we emphasize that this result may imply only that extrinsic damping (e.g., losses from the SQUID loop) dominates.

We conclude that the data presented in Fig. 3 are entirely consistent with thermal activation [Eq. (2)] and, in particular, do not admit an effective barrier height

TABLE I. Characteristic energies (in units of kelvin) of the symmetric double-well potential ($\Phi_x = \frac{1}{2}\Phi_0$) which describes the system for data in Fig. 3. At each temperature Φ_{xdc} has been adjusted to give the values of ΔU shown.

	$T=0.85 \text{ K}$	$T=4.41 \text{ K}$
ΔU	18	92
$\hbar\omega_{lw}$	1.85	3.15
$\hbar\omega_{tw}$	14.6	14.8
$\hbar\omega_{ls}$	1.36	2.61
$\hbar\omega_{ts}$	14.4	14.2
$\Delta U/\hbar\omega_{lw}$	9.7	29
$\Delta U/\hbar\omega_{tw(ts)}$	~ 1.2	~ 6

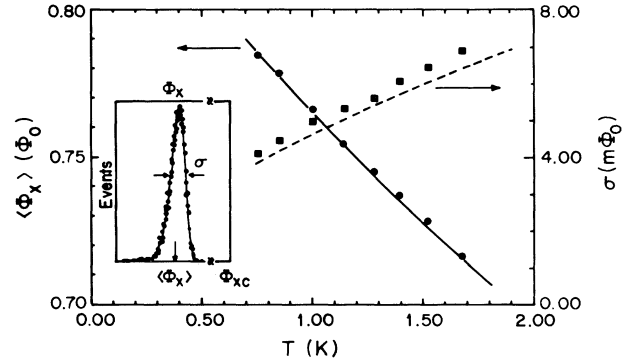


FIG. 4. Mean $\langle \Phi_x \rangle$ (circles) and width σ (squares) of the thermal activation probability distribution (see text) vs T at $\Phi_{xdc} = 0.122\Phi_0$. The solid and dashed lines are, respectively, the predicted mean and width from Eq. (2) using parameters given in text. Inset: A typical distribution used to calculate $\langle \Phi_x \rangle$ and σ at one temperature.

$\Delta U^* = 2.5\Delta U$ as needed by SGV to explain their data in the thermal activation regime. The energies associated with the symmetric potential over the temperature range of the measurements are summarized in Table I. For comparison, we note that both for these data and for those of SGV, $\hbar\omega_l \approx k_B T$, whereas $\hbar\omega_t \gg k_B T$ with $\omega_t/\omega_l \approx 8$. Even for our lowest-temperature data there are at least ten energy levels in the wells, satisfying the validity criteria for the classical [Eq. (2)] and semiclassical¹¹ rate calculations. The expected crossover temperature T_x for tunneling-dominated transitions is $T_x = 0.35 \text{ K}$ in the zero-damping limit. Thus quantum correction¹¹ to Eq. (2) should be negligible for our data. Naor, Tesche, and Ketchen¹² have also reported excellent agreement with thermal activation theory for their measurements for transitions for $T > 1.7 \text{ K}$ in a highly damped, current-biased dc SQUID with $\omega_t/\omega_l \approx 1$.

A more direct comparison with the results of SGV is provided by the data in Fig. 4. Here, for $\Phi_{xdc} = 0.122\Phi_0$, Φ_x is increased at a constant rate reducing the barrier height until the SQUID undergoes a change of fluxoid state by escaping from a metastable well. Measurements of this type on a single-junction SQUID have been described in detail elsewhere.^{9,10} These measurements are repeated approximately 10^4 times at a fixed temperature giving a histogram of transition probability versus Φ_x (see Fig. 4, inset). The first and second moments of this distribution, $\langle \Phi_x \rangle$ and σ , respectively, are predicted to vary with temperature¹³ as shown by the solid and dashed lines in Fig. 4 assuming a potential and transition rate given by Eqs. (1) and (2) and using the sample parameters above.

In calculating $\langle \Phi_x \rangle$ vs T the critical applied flux Φ_{xc} at which $\Delta U = 0$ is used as a temperature-independent fitting parameter, $\Phi_{xc} = 0.882\Phi_0$, which is consistent with β measured for $\Phi_{xdc} = 0$. As can be seen, the agree-

ment with thermal activation predictions is excellent. This contrasts with similar measurements by SGV in which they found for their system that $d\langle\Phi_x\rangle/dT$ was about a factor of 3 less than predicted. The width σ also varies with temperature as expected, although it is about 5% greater than predicted. This is consistent with the excess width expected from the Nyquist flux noise on the sample due to the shunt resistor across the magnetometer. The temperature of this shunt varied from 50 to 180 mK as the sample temperature was increased.

Measurements have been made of thermally activated transitions between fluxoid states of a SQUID system having two macroscopic degrees of freedom, in which the energy potentials could be accurately determined and where existing classical and semiclassical theory should be valid. Excellent agreement has been found with the prediction of thermal activation theory. In particular, no hint was seen of the very large apparent rate suppression recently reported in a similar system by SGV. In view of the similarities of the potentials for these two measurements (in particular, the ratios of the longitudinal and transverse level spacing to $k_B T$), our results should serve to focus on the key features of the system used by SGV responsible for their anomalous results. For example, our results indicate that such anomalies cannot be a general feature of two-dimensional potentials even in the limit where $\hbar\omega_i \gg k_B T$ so that level quantization of the transverse mode is important.

We would like to acknowledge the contributions of C. N. Archie, Aloke Jain, and B. Sen in the initial stages of this work as well as numerous helpful conversations with

S. Chakravarty and S. Kivelson. This work was supported by the U. S. Office of Naval Research.

¹F. Sharifi, J. L. Gavilano, and D. J. Van Harlingen, *Phys. Rev. Lett.* **61**, 742 (1988).

²F. Sharifi, J. L. Gavilano, and D. J. Van Harlingen, *IEEE Trans. Mag.* **25**, 1174 (1989).

³E. Ben-Jacob, D. J. Bergman, Y. Imry, B. J. Matkowsky, and Z. Schuss, *J. Appl. Phys.* **54**, 6533 (1983); C. D. Tesche, *J. Low Temp. Phys.* **44**, 119 (1981).

⁴P. Silvestrini, S. Pagano, Roberto Cristiano, O. Liengme, and K. E. Gray, *Phys. Rev. Lett.* **60**, 844 (1988).

⁵P. Silvestrini, O. Liengme, and K. E. Gray, *Phys. Rev. B* **37**, 1525 (1988).

⁶J. R. Kirtley, C. D. Tesche, W. J. Gallagher, A. W. Kleinsasser, R. L. Sandstrom, S. I. Raider, and M. P. A. Fisher, *Phys. Rev. Lett.* **61**, 2372 (1988).

⁷R. Landauer (private communication); S. Kivelson (private communication).

⁸A. W. Lichtenberger, C. P. McClay, R. J. Mattauch, M. J. Feldman, S. K. Pan, and A. R. Kerr, *IEEE Trans. Mag.* **25**, 1247 (1989).

⁹D. B. Schwartz, B. Sen, C. N. Archie, and J. E. Lukens, *Phys. Rev. Lett.* **55**, 1547 (1985).

¹⁰D. B. Schwartz, Ph.D. thesis, State University of New York at Stony Brook, 1986 (unpublished).

¹¹H. Grabert, P. Olschowski, and Ulrich Weiss, *Phys. Rev. B* **36**, 1931 (1987).

¹²M. Naor, C. D. Tesche, and M. B. Ketchen, *Appl. Phys. Lett.* **41**, 202 (1982).

¹³J. Kurkijärvi, *Phys. Rev. B* **6**, 832 (1972).